Inorg. Chem. **2009**, *48*, 889−901

Ionic Liquids Containing Boron Cluster Anions

Mark Nieuwenhuyzen,[†] Kenneth R. Seddon,[†] Francesc Teixidor,[‡] Alberto V. Puga,[†,‡] and Clara Viñas*[,‡]

Queen's University Ionic Liquid Laboratories (QUILL), The Queen's University of Belfast, David Keir Building, Stranmillis Road, Belfast, Northern Ireland, U.K., BT9 5AG, and Institut de Ciència de Materials de Barcelona (ICMAB-CSIC), Campus UAB, Bellaterra, Barcelona, Spain, E-08193

Received July 31, 2008

The combination of different boron cluster anions and some of the cations typically found in the composition of ionic liquids has been possible by straightforward metathetic reactions, producing new low melting point salts; the imidazolium cations have been systematically studied, $[C_n\text{mim}]^+$ (when $[C_n\text{mim}]^+$ = 1-alkyl-3-methylimidazolium; n = 2, 4, 6, 8, 10, 12, 14, 16, or 18). Melting points increase in the anionic order $[Co(C_2B_9H_{11})_2]^-$ < $[C_2B_9H_{12}]^-$ < $[B_{10}Cl_{10}]^{2-}$ < $[B_{12}Cl_{12}]^{2-}$. Nevertheless, alkyl chain length dramatically influences the thermal behavior, suggesting that packing inefficiency is the main cause of the existence of room temperature ionic liquids. The salts $[C_n\text{mim}][Co(C_2B_9H_{11})_2]$ (n = 4, 6, 8, 10, 12 or 14) are liquids at room temperature, presenting strikingly low glass transition temperatures (≥ −34 °C). The salts $[C_n\text{mim}]_2[X]$ ($[X]^{2-}$ = $[B_{10}Cl_{10}]^{2-}$ or $[B_{12}Cl_{12}]^{2-}$, n = 16 or 18) show liquid crystal phases between the solid and liquid states. Tetraalkylphosphonium salts of $[B_{10}Cl_{10}]^{2-}$ have also been prepared. Physical properties, such as thermal stability, density, or viscosity, have been measured for some selected samples. The presence of the perhalogenated dianion $[B_{12}Cl_{12}]^{2-}$ in the composition of the imidazolium salts renders highly thermally stable compounds. For example, $[C_2\text{mim}]_2[B_{12}Cl_{12}]$ starts to decompose above 480 °C in a dynamic TGA analysis under a dinitrogen atmosphere. Crystal structures of $[C_2\text{mim}][Co(C_2B_9H_{11})_2]$ and $[C_2\text{mim}]_2[B_{12}Cl_{12}]$ have been determined. ^{1}H NMR spectra of selected imidazolium-boron cluster anion salts have been recorded from solutions as a function of the concentration, showing trends related to the cation−anion interactions.

Introduction

In the past decade, hundreds of ionic liquids have been prepared and used mainly as solvents or electrolytes.[1] Furthermore, their interest in other areas of chemistry is burgeoning.[2]

Room-temperature ionic liquids are composed entirely of ions, their compositions frequently being based on an organic cation and a polyatomic inorganic or organic anion. The most widely used cations are imidazolium, pyridinium, ammonium, or phosphonium derivatives bearing at least one alkyl chain. The range of anions found in ionic liquids is large, including the important family of weakly coordinating hydrophobic species, such as $[BF_4]^-$,[3] $[PF_6]^-$,[4] $[NTf_2]^-$ (bis{(trifluoromethyl)sulfonyl}amide),[5] or $[OTf]^-$ (trifluoromethanesulfonate).[5] The number of possible cation−anion combinations is greater than one million,[6] thus allowing the design of tailor-made ionic liquids for a desired task.

Anionic boron clusters are a peculiar class of inorganic anions which exhibit delocalized charge, extraordinarily weak nucleophilicity and relative chemical inertness.[7−9] Deriva-

* To whom correspondence should be addressed. E-mail: clara@icmab.es.
† The Queen's University of Belfast.
‡ Institut de Ciència de Materials de Barcelona (ICMAB-CSIC).

(1) *Ionic Liquids in Synthesis*, 2nd ed.; Wasserscheid, P., Welton, T., Eds.; Wiley-VCH: Weinheim, Germany, 2007.
(2) Plechkova, N. V.; Seddon, K. R. *Chem. Soc. Rev.* **2008**, *37*, 123–150.
(3) Holbrey, J. D.; Seddon, K. R. *J. Chem. Soc., Dalton Trans.* **1999**, 2133–2139.
(4) Gordon, C. M.; Holbrey, J. D.; Kennedy, A. R.; Seddon, K. R. *J. Mater. Chem.* **1998**, *8*, 2627–2636.
(5) Bonhôte, P.; Dias, A. P.; Papageorgiou, N.; Kalyanasundaram, K.; Grätzel, M. *Inorg. Chem.* **1996**, *35*, 1168–1178.
(6) Seddon, K. R. In *The International George Papatheodorou Symposium: Proceedings*; Boghosian, S., Dracopoulos, V., Kontoyannis, C. G., Voyiatzis, G. A., Eds.; Institute of Chemical Engineering and High Temperature Chemical Processes: Patras, Greece, 1999; p 131−135.
(7) Reed, C. A. *Acc. Chem. Res.* **1998**, *31*, 133–139.
(8) Strauss, S. H. *Chem. Rev.* **1993**, *93*, 927–942.
(9) Krossing, I.; Raabe, I. *Angew. Chem., Int. Ed.* **2004**, *43*, 2066–2090.

10.1021/ic801448w CCC: $40.75
Published on Web 01/07/2009

tives of the monocarborane [*closo*-$CB_{11}H_{12}]^-$ anion have provided excellent results in the stabilization of complex cations,[7,8,10] strong electrophiles,[7,11,12] and superacids.[7,12,13] Despite their stability, boron cluster anions can be functionalized to obtain several derivatives with different kinds and degrees of substitution.

During the current decade, the first ionic liquids where the anion is a boron cluster have been prepared. Reed and co-workers reported the synthesis and characterization of imidazolium salts with [*closo*-$CB_{11}H_{12}]^-$ derivatives, whose melting points were as low as 45 °C.[14] Some years later, Wesemann and co-workers introduced stannaboranes ([1-R-*closo*-$SnB_{11}H_{11}]^-$) in similar salts.[15] Zhu et al. reported the preparation of the 1-pentylpyridinium salt of [*closo*-$CB_{11}H_{12}]^-$ (mp = 19 °C).[16] More recently, [*nido*-$C_2B_9H_{12}]^-$ has proved to depress melting points compared to [*closo*-$CB_{11}H_{12}]^-$,[17] whereas Gabel and co-workers reported that, when using [*closo*-$B_{12}H_{11}NR_3]^-$ anions (R = alkyl), a wide range of cations can yield room temperature ionic liquids, even Li^+ or H^+.[18]

In this study, we have systematically combined either imidazolium or phosphonium cations with four boron cluster anions, that is, the cobaltabis(dicarbollide) [*commo*-3,3′-Co(1,2-$C_2B_9H_{11})_2]^-$, [*nido*-$C_2B_9H_{12}]^-$, and two perhalogenated dianions: [*closo*-$B_{12}Cl_{12}]^{2-}$ and [*closo*-$B_{10}Cl_{10}]^{2-}$ (see Chart 1). They will be abbreviated in this paper as [Co($C_2B_9H_{11})_2]^-$, [$C_2B_9H_{12}]^-$, [$B_{12}Cl_{12}]^{2-}$, and [$B_{10}Cl_{10}]^{2-}$, respectively. In addition to the investigations on phase-transition temperatures and phase diagrams, other important properties, such as decomposition temperatures, density, and viscosity, have been explored for these substances. Detailed spectroscopic data have also been recorded, suggesting some trends in the structure of cations and anions in solution.

Chart 1. Boron Cluster Anions and 1-Alkyl-3-methylimidazolium and Tetraalkylphosphonium Cations Used in This Study[a]

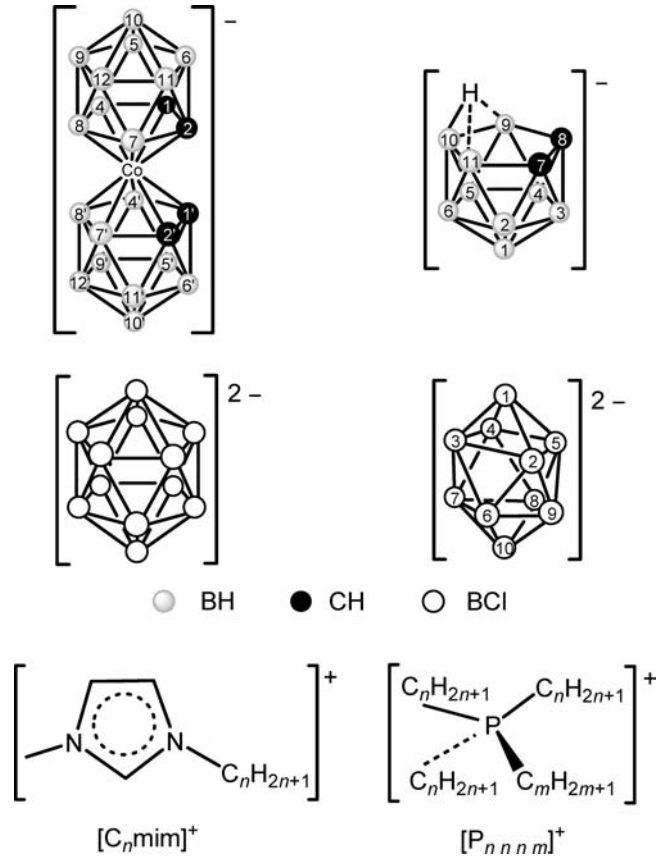

[a] Numbering scheme is shown for boron vertices.

Experimental Section

[$C_n$mim]Cl,[19,20] [$P_{n\ n\ n\ m}$]Cl,[21] and [$NHMe_3$][$C_2B_9H_{12}$][22] were synthesized as previously reported. 1,2-*closo*-$C_2B_{10}H_{12}$, Cs[Co($C_2B_9H_{12})_2$], [NH_4]$_2$[$B_{12}Cl_{12}$],[23] and [NH_4]$_2$[$B_{10}Cl_{10}$] were purchased from Katchem Ltd. and used as received. Organic solvents were purchased as reagent grade and used as received.

All metathetic reactions were carried out under standard laboratory conditions. Nevertheless, [C_2mim]Cl, [C_4mim]Cl and [C_6mim]Cl were stored and weighted inside a Kewaunee Scientific Corp. inert atmosphere (N_2) glovebox (O_2, H_2O < 1 ppm). Elemental analyses were performed using a Carlo Erba EA1108

(10) (a) Moxham, G. L.; Douglas, T. M.; Brayshaw, S. K.; Kociok-Köhn, G.; Lowe, J. P.; Weller, A. S. *Dalton Trans.* **2006**, 5492–5505. (b) Douvris, C.; Reed, C. A. *Organometallics* **2008**, *27*, 807–810. (c) Douglas, T. M.; Molinos, E.; Brayshaw, S. K.; Weller, A. S. *Organometallics* **2007**, *26*, 463–465.

(11) (a) Reed, C. A. *Acc. Chem. Res.* **1998**, *31*, 325–332. (b) Reed, C. A.; Kim, K. C.; Stoyanov, E. S.; Stasko, D.; Tham, F. S.; Mueller, L. J.; Boyd, P. D W. *J. Am. Chem. Soc.* **2003**, *125*, 1796–1804. (c) Kato, T.; Reed, C. A. *Angew. Chem., Int. Ed.* **2004**, *43*, 2908–2911. (d) Kato, T.; Stoyanov, E.; Geier, J.; Grutzmacher, H.; Reed, C. A. *J. Am. Chem. Soc.* **2004**, *126*, 12451–12457. (e) Stasko, D.; Reed, C. A. *J. Am. Chem. Soc.* **2002**, *124*, 1148–1149. (f) Douvris, C.; Stoyanov, E. S.; Tham, F. S.; Reed, C. A. *Chem. Commun.* **2007**, 1145–1147. (g) Hoffmann, S. P.; Kato, T.; Tham, F. S.; Reed, C. A. *Chem. Commun.* **2006**, 767–769.

(12) (a) Zhang, Y.; Tham, T. S.; Nixon, J. F.; Taylor, C.; Green, J. C.; Reed, C. A. *Angew. Chem., Int. Ed.* **2008**, *47*, 3801–3804. (b) Zhang, Y.; Tham, F. S.; Reed, C. A. *Inorg. Chem.* **2006**, *45*, 10446–10448.

(13) (a) Juhasz, M.; Hoffmann, S.; Stoyanov, E.; Kim, K. C.; Reed, C. A. *Angew. Chem., Int. Ed.* **2004**, *43*, 5352–5355. (b) Reed, C. A. *Chem. Commun.* **2005**, 1669–1677. (c) Stoyanov, E. S.; Kim, K. C.; Reed, C. A. *J. Am. Chem. Soc.* **2006**, *128*, 8500–8508. (d) Stoyanov, E. S.; Hoffmann, S. P.; Juhasz, M.; Reed, C. A. *J. Am. Chem. Soc.* **2006**, *128*, 3160–3161.

(14) Larsen, A. S.; Holbrey, J. D.; Tham, F. S.; Reed, C. A. *J. Am. Chem. Soc.* **2000**, *122*, 7264–7272.

(15) Ronig, B.; Pantenburg, I.; Wesemann, L. *Eur. J. Inorg. Chem.* **2002**, *31*, 9–322.

(16) Zhu, Y. H.; Ching, C. B.; Carpenter, K.; Xu, R.; Selvaratnam, S.; Hosmane, N. S.; Maguire, J. A. *Appl. Organomet. Chem.* **2003**, *17*, 346–350.

(17) Dymon, J.; Wibby, R.; Kleingardner, J.; Tanski, J. M.; Guzei, I. A.; Holbrey, J. D.; Larsen, A. S. *Dalton Trans.* **2008**, 2999–3006.

(18) Justus, E.; Rischka, M.; Wishart, J. F.; Werner, K.; Gabel, D. *Chem.—Eur. J.* **2008**, *14*, 1918–1923.

(19) (a) Wilkes, J. S.; Levisky, J. A.; Wilson, R. A.; Hussey, C. L. *Inorg. Chem.* **1982**, *21*, 1263–1264. (b) Deetlefs, M.; Seddon, K. R. *Green Chem.* **2003**, *5*, 181–186. (c) Dyson, P. J.; Grossel, M. C.; Srinivasan, N.; Vine, T.; Welton, T.; Williams, D. J.; White, A. J. P.; Zigras, T. *J. Chem. Soc., Dalton Trans.* **1997**, 3465–3469.

(20) Avent, A. G.; Chaloner, P. A.; Day, M. P.; Seddon, K. R.; Welton, T. *J. Chem. Soc., Dalton Trans.* **1994**, 3405–3413.

(21) Bradaric, C. J.; Downard, A.; Kennedy, C.; Robertson, A. J.; Zhou, Y. H. *Green Chem.* **2003**, *5*, 143–152.

(22) (a) Wiesboeck, R. A.; Hawthorne, M. F. *J. Am. Chem. Soc.* **1964**, *86*, 1642. (b) Hawthorne, M. F.; Young, D. C.; Garrett, P. M.; Owen, D. A.; Schwerin, S. G.; Tebbe, F. N.; Wegner, P. A. *J. Am. Chem. Soc.* **1968**, *90*, 862.

(23) The commercial [NH_4]$_2$[$B_{12}Cl_{12}$] appeared to be incompletely chlorinated. The actual composition was determined to be [NH_4]$_2$[$B_{12}Cl_{11.7}H_{0.3}$] on the basis of the integration of the peaks in the ^{11}B NMR spectrum (see Supporting Information). However, the salt was used without further purification.

Table 1. DSC, Optical Microscopy, and TGA data[a]

		Heating		Cooling		
	synthetic method	T_m/°C (ΔH/kJ mol^{-1})	T_g/°C (ΔH/kJ mol^{-1})	T_g'/°C (ΔH/kJ mol^{-1})	T_f/°C (ΔH/kJ mol^{-1})	T_d/°C
$[C_2mim][Co(C_2B_9H_{11})_2]$	A	113 (22.1)			*c*	
$[C_4mim][Co(C_2B_9H_{11})_2]$	A	−18[b]			*c,d*	340
$[C_6mim][Co(C_2B_9H_{11})_2]$	A	−23[b]			*c,d*	
$[C_8mim][Co(C_2B_9H_{11})_2]$	A	−28[b]			*c,d*	
$[C_{10}mim][Co(C_2B_9H_{11})_2]$	A	−32[b]			*c,d*	
$[C_{12}mim][Co(C_2B_9H_{11})_2]$	A	−34[b]			*c,d*	
$[C_{14}mim][Co(C_2B_9H_{11})_2]$	A	−34[b]			*c,d*	
$[C_{16}mim][Co(C_2B_9H_{11})_2]$	A	58 (16.7)			*c*	
$[C_{18}mim][Co(C_2B_9H_{11})_2]$	A	66 (53.4)			*c*	
$[C_2mim][C_2B_9H_{12}]$	B1	98 (10.1)			79 (−12.2)	
$[C_4mim][C_2B_9H_{12}]$	B1,B2	43 (17.4)			*c*	280
$[C_6mim][C_2B_9H_{12}]$	B1	65 (17.3)			*c*	
$[C_8mim][C_2B_9H_{12}]$	B1	47 (13.7)			*c*	
$[C_{10}mim][C_2B_9H_{12}]$	B1	52 (13.5)			*c*	
$[C_{12}mim][C_2B_9H_{12}]$	B1	68 (24.1)			29 (−26.4)	
$[C_{14}mim][C_2B_9H_{12}]$	B1	73 (28.4)			27 (−34.9)	
$[C_{16}mim][C_2B_9H_{12}]$	B1	76 (28.8)			42 (−37.0)	
$[C_{18}mim][C_2B_9H_{12}]$	B1,B2	83 (42.4)			63 (−47.4)	
$[C_2mim]_2[B_{10}Cl_{10}]$	C	124 (13.7)[e]	229 (6.0)	218 (−6.2)[e]	78 (−10.0)	440
$[C_8mim]_2[B_{10}Cl_{10}]$	C	126 (5.5)			92 (−1.2)	
$[C_{16}mim]_2[B_{10}Cl_{10}]$	C	71 (43.0)	125 (0.9)	121 (−0.8)	*c*	
$[C_{18}mim]_2[B_{10}Cl_{10}]$	C	81 (48.1)	139 (0.8)	131 (−0.7)	*c*	380
$[C_2mim]_2[B_{12}Cl_{12}]$	D	265 (20.8)[e]	304 (7.9)	277 (−6.8)[e]	221 (−26.4)	480
$[C_8mim]_2[B_{12}Cl_{12}]$	D	127 (11.1)			107 (−10.2)	
$[C_{10}mim]_2[B_{12}Cl_{12}]$	D	174 (17.4)			129 (−19.6)	
$[C_{16}mim]_2[B_{12}Cl_{12}]$	D	105 (21.2)	150 (2.2)	149[f]	98 (−17.7)	
$[C_{18}mim]_2[B_{12}Cl_{12}]$	D	110 (15.6)	157 (2.0)	152[f]	100 (−16.9)	
$[P_{5\,5\,5\,6}]_2[B_{10}Cl_{10}]$	E	239 (13.0)			211 (12.9)	
$[P_{6\,6\,6\,14}]_2[B_{10}Cl_{10}]$	E	53[e]			*c*	

[a] Melting (T_m) and clearing points (T_g) were recorded during the second heating cycle in the DSC traces and checked by heated stage optical microscopy. Liquid−mesophase transition temperatures (T_g') and freezing temperatures (T_f) were recorded during the second cooling cycle in the DSC traces. Decomposition temperatures (T_d) under a dinitrogen atmosphere were determined from the onset of weight loss in the TGA traces. [b] Second-order glass transition. [c] Did not crystallize upon cooling. [d] A change in the heat flow slopes was observed in the cooling cycles at temperatures very close to the corresponding glass transition temperatures. [e] These samples did not form a liquid crystalline mesophase, but a glassy state. [f] Enthalpy changes too small to be accurately measured.

microanalyser. For liquid samples, IR spectra were recorded from thin films on NaCl discs in a Shimadzu FTIR-8300 spectrophotometer, whereas some selected solid samples were analyzed by attenuated total reflection (ATR) on a Bruker Tensor 27 single reflection diamond ATR instrument. All salts were also measured as KBr pellets. ^{1}H NMR (300.13 MHz), ^{11}B NMR (96.29 MHz), and ^{13}C NMR (75.47 MHz) spectra were recorded on a Bruker ARX 300 spectrometer. Chemical shift values for ^{11}B NMR spectra were referenced to external $BF_3 \cdot OEt_2$, and those for ^{1}H and ^{13}C NMR spectra were referenced to $SiMe_4$. The melting points and other transition temperatures for solid samples were determined by differential scanning calorimetry (DSC), at 10 °C min^{-1} heating/cooling rates on 5−10 mg samples on a Perkin-Elmer Pyris 7 DSC instrument and by heated-stage polarizing optical microscopy using an Olympus BX50 microscope equipped with a Linkam TH600 hot stage and TP92 temperature controller. Data for the liquid samples were recorded on a Perkin-Elmer Pyris 1 DSC instrument equipped with dinitrogen cryostatic cooling, at 10 °C min^{-1} heating/cooling rates. DSC apparati were calibrated using indium or cyclohexane as standards. Quoted values were taken from the first peak of the second heating cycle in the DSC traces. Thermogravimetric analyses (TGA) were performed for 5−10 mg samples in platinum pans, using a Perkin-Elmer Pyris 1 thermogravimetric analyzer under a dinitrogen atmosphere, at 5 °C min^{-1} heating rate. Density values were determined using an Anton Paar 4500 oscillating densimeter. Viscosity measurements have been made on a Brookfield DV II+ cone and plate viscosity meter. Electronic absorption spectra were recorded in a Shimadzu Pharma Specc UV-1700 UV−visible spectrophotometer.

^{1}H and ^{13}C{^{1}H} NMR data, CHN microanalyses, viscosity and density data, and examples of actual NMR and FT-IR spectra for selected samples are presented in the Supporting Information. Transition temperatures and decomposition temperatures (where determined) are given in Table 1. Typical synthetic procedures for the preparation of the newly synthesized salts are described below.

$[C_n mim][Co(C_2B_9H_{11})_2]$ (Method A). $[C_2mim]Cl$ (133 mg, 0.907 mmol) was dissolved in a dichloromethane/propanone mixture (6:1 by volume, 10 cm^3) and added to the stirred solution of $Cs[Co(C_2B_9H_{11})_2]$ (414 mg, 0.907 mmol) in the same solvent mixture (20 cm^3). A white precipitate appeared immediately. After the mixture was stirred for 4 h, the solid was removed by filtration through Celite, and the solution was evaporated to dryness under reduced pressure. The resulting orange solid was dried in vacuo for 12 h at 100 °C, yielding $[C_2mim][Co(C_2B_9H_{11})_2]$ (393 mg, 99.6%). Yields for $[C_n mim][Co(C_2B_9H_{11})_2]$ with $n = 4-18$ were in the 99−100% range. For $[C_n mim][Co(C_2B_9H_{11})_2]$ with $n = 4$, 6, 8, 10, 12, and 14, the resulting products were deep red viscous liquids, whereas they were orange solids for $n = 2$, 16, and 18.

Orange crystals suitable for single-crystal X-ray crystallography were grown for $[C_2mim][Co(C_2B_9H_{11})_2]$ from trichloromethane solutions by slow evaporation at 5 °C.

$[C_n mim][C_2B_9H_{12}]$ (Method B). Method B1. $[C_2mim]Cl$ (128 mg, 0.873 mmol) was dissolved in a water/methanol mixture (4:5 by volume, 10 cm^3) and added to the stirred solution of $[NHMe_3][C_2B_9H_{12}]$ (169 mg, 0.873 mmol) in the same solvent mixture (20 cm^3). After the mixture was stirred for 4 h, the solution was concentrated to half of its volume in a rotary evaporator at reduced pressure. The white precipitate formed was collected by

filtration under reduced pressure, washed with water (3 × 5 cm^3), and dried in vacuo for 12 h at 100 °C, yielding [C_2mim][$C_2B_9H_{12}$] (138 mg, 65%). For [$C_n$mim][$C_2B_9H_{12}$] with n = 4, 6, 8, 10, 12, 14, 16, and 18, the solution became cloudy immediately during the mixing of the reagents. The longer the alkyl chain, the higher the yields, up to 90%.

Method B2. KOH (85% w/w, 0.967 g, 14.6 mmol) was dissolved in degassed ethanol (12.5 cm^3); 1,2-*closo*-$C_2B_{10}H_{12}$ (500 mg, 3.47 mmol) was added, and the solution was heated under reflux under dinitrogen for 3 h. Afterward, volatiles were removed in vacuo, and the residue was dissolved in water (20 cm^3). A solution of [C_4mim]Cl (610 mg, 3.49 mmol) in water (10 cm^3) was added, and the white precipitate thus formed was collected by filtration, rinsed with water (3 × 5 cm^3), and dried in vacuo for 12 h to give [C_4mim][$C_2B_9H_{12}$] (917 mg, 97% based on carborane).

[$C_n$mim]$_2$[$B_{10}Cl_{10}$] (Method C). [C_2mim]Cl (130 mg, 0.887 mmol) was dissolved in water (10 cm^3) and added to a stirred solution of [NH_4]$_2$[$B_{10}Cl_{10}$] (221 mg, 0.443 mmol) in water (20 cm^3). The solution immediately became cloudy. After 4 h of stirring, the white solid was collected by filtration under reduced pressure, washed with water (3 × 5 cm^3), and dried in vacuo for 12 h at 100 °C, yielding [C_2mim]$_2$[$B_{10}Cl_{10}$] as a white solid (281 mg, 93%).

[$C_n$mim]$_2$[$B_{12}Cl_{12}$] (Method D). [C_2mim]Cl (127 mg, 0.866 mmol) was dissolved in water (10 cm^3) and added to a stirred solution of [NH_4]$_2$[$B_{12}Cl_{12}$] (256 mg, 0.433 mmol) in water (20 cm^3). The solution immediately became cloudy. After the mixture was stirred for 4 h, the white solid was collected by filtration under reduced pressure, washed with water (3 × 5 cm^3), and dried in vacuo for 12 h at 100 °C, yielding [C_2mim]$_2$[$B_{12}Cl_{12}$] as a white solid (318 mg, 95%).

Crystals suitable for single-crystal X-ray crystallography were grown for [C_2mim]$_2$[$B_{12}Cl_{12}$] from ethanenitrile solution by slow evaporation at 5 °C.

[$P_{n\ n\ n\ m}$]$_2$[$B_{10}Cl_{10}$] (Method E). [$P_{6\,6\,6\,14}$]Cl (444 mg, 0.855 mmol) was dissolved in a methanol/water mixture (3:1 by volume, 10 cm^3) and added to a stirred solution of [NH_4]$_2$[$B_{10}Cl_{10}$] (213 mg, 0.427 mmol) in the same solvent mixture (20 cm^3). The solution immediately became cloudy. After 4 h of stirring, the white waxy solid was allowed to settle and was decanted, washed with a hot methanol/water mixture (3:1 by volume, 3 × 5 cm^3), and dried in vacuo for 12 h at 100 °C, yielding [$P_{6\,6\,6\,14}$]$_2$[$B_{10}Cl_{10}$] (490 mg, 80%). [$P_{5\,5\,5\,6}$]$_2$[$B_{10}Cl_{10}$] was prepared from a methanol/water mixture (1:2 by volume) in 80% yield.

Crystallographic Details. Crystal data for each structure are given below. A crystal was mounted on to the diffractometer at low temperature under dinitrogen at 173 K. The structures were solved using direct methods and refined with the SHELXTL version 5, and the non-hydrogen atoms were refined with anisotropic thermal parameters. Hydrogen-atom positions were added at idealized positions with a riding model and fixed thermal parameters (U_{ij} = 1.2U_{eq} (1.5 for methyl) for the atom to which they are bonded). The function minimized was $\Sigma[w(|F_o|^2 - |F_c|^2)]$ with reflection weights $w^{-1} = [\sigma^2 |F_o|^2 + (g_1P)^2 + (g_2P)]$, where $P = [\max|F_o|^2 + 2|F_c|^2]/3$. Additional material available from the Cambridge Crystallographic Data Centre (CCDC-708849 and CCDC-708850) comprises relevant tables of atomic coordinates, bond lengths and angles, and thermal parameters.

Crystal data for [C_2mim]$_2$[$B_{12}Cl_{12}$] ($C_{12}H_{22}B_{12}Cl_{12}N_2$): $-M$ = 777.46, triclinic, space group $P\bar{1}$, a = 9.3744(13) Å, b = 9.6448(14) Å, c = 9.9629(14) Å, α = 105.120(2)°, β = 104.023(2)°, γ = 102.275(2)°, U = 806.3 (2) Å^3, Z = 1, μ = 1.047 mm^{-1}, R_{int} = 0.1767. A total of 4588 reflections were measured for the angle range 4 < 2θ < 45, and 2831 independent reflections were used in the refinement. The final parameters were wR2 = 0.1772 and R1 = 0.0604 [$I > 2\sigma I$].

Crystal data for [C_2mim][Co($C_2B_9H_{11}$)$_2$] ($C_{10}H_{33}B_{18}CoN_2$): $-M$ = 434.89, monoclinic, space group $P2_1$, a = 10.5411(10) Å, b = 20.8825(18) Å, c = 10.6300(4) Å, β = 96.8740(10)°, U = 2323.1 (4) Å^3, Z = 4, μ = 0.741 mm^{-1}, R_{int} = 0.0669. A total of 16 363 reflections were measured for the angle range 3.8 < 2θ < 57, and 10 674 independent reflections were used in the refinement. The final parameters were wR2 = 0.1140 and R1 = 0.0448 [$I > 2\sigma I$].

Search procedures in Cambridge Structural Database (CSD) were done using ConQuest (version 5.29).[24] The CSD (updated January 2008), was examined using the following criteria: 3D coordinates determined, not disordered crystal structures, with no errors and no powder structures. The R factor was set to be below 5%.

Results and Discussion

Synthesis. The salts were prepared by conventional metathetic reactions; Chart 1 shows the structures of the anions and cations involved. The four precursors used were Cs[Co($C_2B_9H_{11}$)$_2$], [$NHMe_3$][$C_2B_9H_{12}$], [NH_4]$_2$[$B_{12}Cl_{12}$], and [NH_4]$_2$[$B_{10}Cl_{10}$]. Solvents were selected appropriate to their different solubilities, and those of the imidazolium or phosphonium chlorides.

1-Alkyl-3-methylimidazolium salts of the cobaltabis(dicarbollide) [Co($C_2B_9H_{11}$)$_2$]$^-$ could be obtained in excellent yields by reaction of Cs[Co($C_2B_9H_{11}$)$_2$] and [$C_n$mim]Cl in dichloromethane/propanone (6:1 by volume; method A). Reed and co-workers previously reported these conditions to be very efficient for the preparation of related imidazolium monocarborane salts (monocarborane = [*closo*-$CB_{11}H_{12}$]$^-$ derivative).[14] The solid CsCl formed was removed by a simple filtration. After removal of volatiles under reduced pressure, [$C_n$mim][Co($C_2B_9H_{11}$)$_2$] were obtained as orange crystalline solids for n = 2, 16, or 18 but, surprisingly, as dark red viscous transparent liquids for the rest of the cases, that is, for n = 4, 6, 8, 10, 12, or 14.

For the anion [*nido*-$C_2B_9H_{12}$]$^-$, where trimethylammonium was the counteranion (method B1), a 5:4 methanol/water mixture was used as the solvent. The imidazolium *nido*-carborane salts precipitated from the mixture, but not quantitatively in all cases: especially the shortest alkyl chain imidazolium salts were observed to be too soluble, and concentration under reduced pressure was needed prior to filtration, without observing a decrease in purity. Yields were good to high, the longest n in [$C_n$mim]$^+$ giving the highest yield. The trimethylammonium salt was used because of its ease of purification and handling, but a procedure in aqueous solution starting from an alkali metal salt of the *nido*-carborane also proved convenient. So, if the metathetic reaction is carried out immediately after the partial degradation of 1,2-*closo*-$C_2B_{10}H_{12}$,[22] where the potassium salt K[$C_2B_9H_{12}$] is produced (method B2), yields increase to 97% and the trimethylammonium salt isolation step is avoided.

The dinegative perchlorinated *closo*-borates were available in water-soluble forms: [NH_4]$_2$[$B_{12}Cl_{12}$] and [NH_4]$_2$[$B_{10}Cl_{10}$].

(24) Allen, F. H.; Motherwell, W. D. S. *Acta Crystallogr. B* **2002**, *58*, 407–422. (a) Allen, F. H. *Acta Crystallogr. B* **2002**, *58*, 380–388.

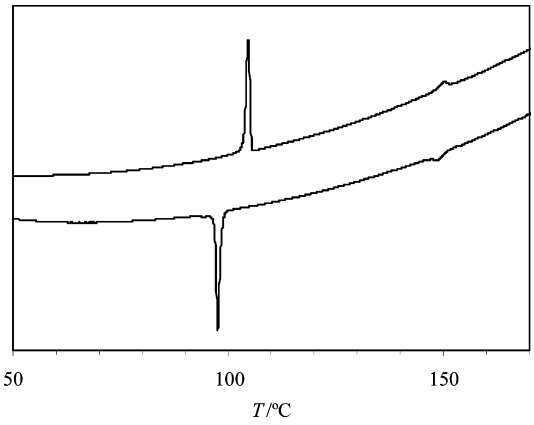

Figure 1. DSC curve of $[C_{16}mim]_2[B_{12}Cl_{12}]$ for the second heating (upper) and cooling (lower) cycles at 10 °C min^{-1} heating/cooling rate. The sharp intense crystal−mesophase and the weak mesophase−liquid transitions can be observed.

Thus, simple reaction in aqueous solution with the corresponding imidazolium chlorides yielded the desired salts as insoluble white solids (methods C and D). The phosphonium perchloro-*closo*-borate salts, $[P_{6\,6\,6\,14}]_2[B_{10}Cl_{10}]$ and $[P_{5\,5\,5\,6}]_2$-$[B_{10}Cl_{10}]$, were generated as insoluble solids from methanol/water mixtures (method E). Methanol was added because of the low solubility of the starting phosphonium chloride in water.

The prepared salts were dried in vacuo at 100 °C. Nevertheless, they are not especially hygroscopic and, for most purposes, can be handled and stored in air. This property makes them attractive for application purposes.

Trends in Melting Points. The phase transition temperatures and related enthalpy changes for the prepared imidazolium or phosphonium boron cluster anion salts are presented in Table 1. Most of the samples showed only one transition, from the solid state to the isotropic liquid, but some form intermediate thermotropic mesophases. The glass transition temperatures, melting points, and clearing points are given from the second heating cycles in the DSC measurements; the liquid-mesophase transition temperatures and freezing points are given from the second cooling cycles. All the samples without exception showed some tendency to supercool. Some of them did not crystallize immediately after the first cooling cycle, so they were allowed to solidify at room temperature for several hours, and then rerecorded. Heated stage optical microscopy confirmed the melting points and mesophase formation temperatures (as appropriate). The observed transition temperatures measured on heating were, in all cases, within ±1 °C of those given by the DSC analyses. The DSC curve of $[C_{16}mim]_2[B_{12}Cl_{12}]$ is depicted in Figure 1, as a representative example.

The newly synthesized imidazolium-boron cluster anion salts can be divided into two distinguishable groups, depending on their thermal behavior. Those in which the anion is monovalent, $[Co(C_2B_9H_{11})_2]^-$ or $[C_2B_9H_{12}]^-$, were found to melt at relatively low temperatures, around or below 100 °C, and did not form thermotropic mesophases. Special mention must be given to $[C_nmim][Co(C_2B_9H_{11})_2]$ with n = 4, 6, 8, 10, 12, or 14 (vide infra), which are liquids at room temperature. In contrast, imidazolium salts with dinegative

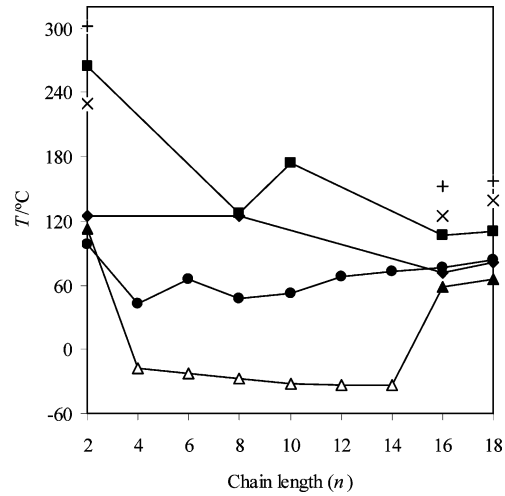

Figure 2. Melting points (closed symbols), glass transition temperatures (open symbols), and clearing points (+, ×) for $[C_nmim]^+$ salts of $[B_{12}Cl_{12}]^{2-}$ (■, +), $[B_{10}Cl_{10}]^{2-}$ (♦, ×), $[C_2B_9H_{12}]^-$ (•), and $[Co(C_2B_9H_{11})_2]^-$ (▲).

perchlorinated *closo*-borate dianions, $[B_{12}Cl_{12}]^{2-}$ or $[B_{10}Cl_{10}]^{2-}$, showed higher melting points; this, of course, is in accord with the Kapustinskii equation, which shows higher Coulombic attraction for doubly charged ions and, in turn, higher melting enthalpy,[25] but thermotropic mesophases were observed for those with longer alkyl chains, possibly because of microphase segregation.

Investigations on imidazolium monocarborane salts suggested that packing inefficiency is the major cause in lowering melting points.[14] This clearly agrees with the trends observed for the cobaltabis(dicarbollide) salts presented here. When the chain length in the 1-alkyl-3-methylimidazolium cation is varied, the thermal properties of $[C_nmim]$-$[Co(C_2B_9H_{11})_2]$ experience drastic changes. The salt with the shortest alkyl chain, n = 2, is a crystalline solid which melts at 113 °C; but surprisingly, those with n = 4, 6, 8, 10, 12, or 14 are viscous liquids at room temperature, unable to crystallize upon cooling, but progressively becoming more viscous liquids and finally glasses. Glass transition temperatures of the above-mentioned salts, determined by DSC, fall within the −18 to −34 °C range (see Figure 2 and Table 1). The members with n = 16 or 18 are obtained as crystalline solids at room temperature; enhanced Van der Waals interactions could be increasing their lattice energies. It should be noted that $[C_nmim][Co(C_2B_9H_{11})_2]$ with n = 4, 6, 8, 10, 12, or 14 become liquids at temperatures around 100 °C lower than the analogues with anions based on icosahedral structures.[14,15,17,18] The reason for this marked decrease is most probably related to the higher molecular volume of the cobaltabis(dicarbollide) anion, more than double those of the other anions named above, implying a more dispersed charge. This cobaltabis(dicarbollide) anion has been used as doping agent in conducting organic polymers, providing high overoxidation resistance, charge reversibility and stability to oxidation−reduction cycles;[26]

(25) Kapustinskii, A. F. *Quart. Rev.* **1956**, *10*, 283–294.
(26) (a) Masalles, C.; Borros, S.; Viñas, C.; Teixidor, F. *Adv. Mater.* **2000**, *12*, 1199–1202. (b) David, V.; Viñas, C.; Teixidor, F. *Polymer* **2006**, *47*, 4694–4702.

also the improvement in the properties of these materials has been ascribed to the low charge density of the anion.[27]

For the crystalline solids, $[C_n\text{mim}][Co(C_2B_9H_{11})_2]$ with $n = 2$, 16, or 18, enthalpy changes are relatively large (>15 kJ mol^{-1}, see Table 1). These values are similar to those published for 1-alkyl-3-methylimidazolium[3,4,28,29] and 1-alkylpyridinium[4,29] salts indicative of a significant structural change, often related with melting transitions. In contrast, second-order glass transitions are observed for the room-temperature liquid salts, that is, $[C_n\text{mim}][Co(C_2B_9H_{11})_2]$ with $n = 4$, 6, 8, 10, 12, or 14.

The salts of the [*nido*-$C_2B_9H_{12}]^-$ anion are crystalline solids at room temperature, but all their melting points are below 100 °C. The chain length of the imidazolium cation also plays an important role on the thermal behavior of these substances, but not as dramatically as for the cobaltabis(dicarbollide) anion discussed above. The melting points are in the range of 43−98 °C (see Figure 2). The largest difference is that from $n = 2$ to $n = 4$, as for $[Co(C_2B_9H_{11})_2]^-$. Enthalpy changes are still significant (>10 kJ mol^{-1}), in general increasing with the alkyl chain length. This is in agreement with a transition from a crystalline phase to the liquid state, as was also observed by hot stage optical microscopy.

The imidazolium salts with dinegative perchlorinated *closo*-borate dianions, $[C_n\text{mim}]_2[B_{12}Cl_{12}]$ and $[C_n\text{mim}]_2[B_{10}Cl_{10}]$, melt at temperatures substantially higher (in general) than the ones with monovalent anions described above, as expected from the Kapustinskii equation, and the related melting enthalpy.[25] Both the higher symmetry in the anion and the enhanced electrostatic forces could increase the lattice energy. Moreover, liquid crystalline mesomorphism is observed for $n = 16$ or 18 before melting (see Table 1 and Figure 2). An example of DSC trace for $[C_{16}\text{mim}]_2[B_{12}Cl_{12}]$ is shown in Figure 1. The presence of the liquid crystalline phase was observed on both cooling from the isotropic liquid and heating from the crystalline solid. When these samples are cooled from the isotropic liquid between two glass microscope slides, a focal conic texture is observed under crossed polarisers (Figure 3). This feature is quite general for imidazolium salts with at least one long unbranched alkyl chain, and has been related to the presence of a smectic A (S_A) phase.[29,30] $[C_2\text{mim}]_2[B_{12}Cl_{12}]$ and $[C_2\text{mim}]_2[B_{10}Cl_{10}]$ do not form any liquid crystalline phase but a plastic glassy state before melting, as suggested by optical microscopy.

Quaternary phosphonium salts of $[B_{10}Cl_{10}]^{2-}$ were prepared to check how the change of cation affects the thermal properties. The melting point of $[P_{6\,6\,6\,14}]_2[B_{10}Cl_{10}]$ was 53 °C, whereas that of $[P_{5\,5\,5\,6}]_2[B_{10}Cl_{10}]$ was 239 °C. As for tetraalkylammonium salts,[31] melting points decrease in general when increasing the cation size for a given anion.

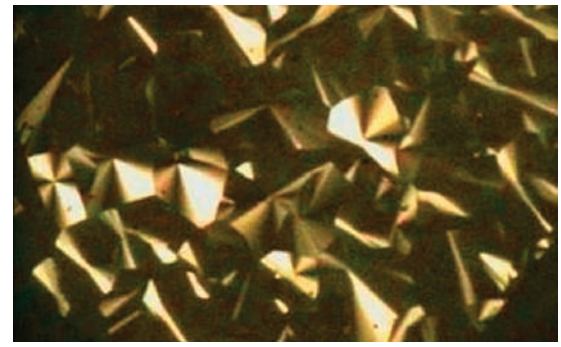

Figure 3. Focal conic texture of the mesophase of $[C_{16}\text{mim}]_2[B_{10}Cl_{10}]$ under crossed polarizers at 85 °C.

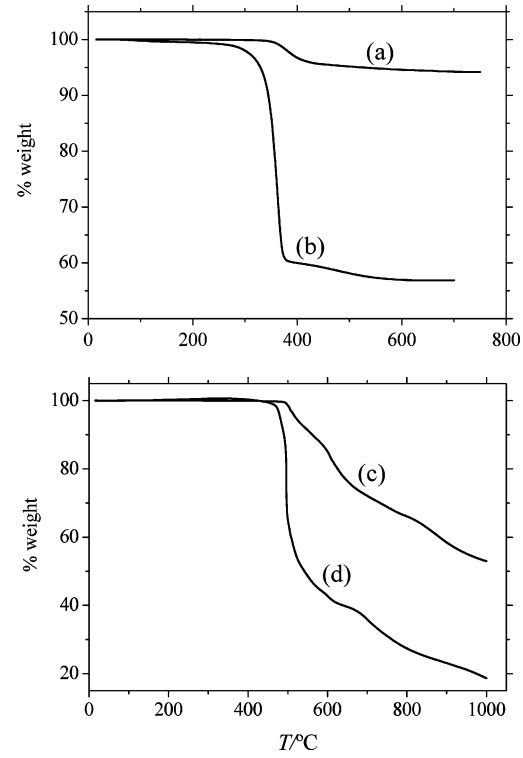

Figure 4. TGA curves for (a) $[C_4\text{mim}][Co(C_2B_9H_{11})_2]$, (b) $[C_4\text{mim}][C_2B_9H_{12}]$, (c) $[C_2\text{mim}]_2[B_{12}Cl_{12}]$, and (d) $[C_2\text{mim}]_2[B_{10}Cl_{10}]$ under a dinitrogen atmosphere at 5 °C min^{-1} heating rate.

This can be rationalized by the increase of interionic separation, and the consequent weakening of electrostatic forces.[25] Thus, the generation of ionic liquids is still possible with bulky perhalogenated *closo*-borate anions, but a careful choice of the cation is essential.

Thermal Stability of Imidazolium Salts. Thermogravimetric analysis curves for representative samples under a dinitrogen atmosphere are shown in Figure 4. Decomposition temperatures, taken from the onset of weight loss, are listed in Table 1. It should be noted that these are dynamic data; static decomposition temperatures may be considerably lower.[32] Thermal stability appears to be strongly dependent on the anion, increasing for the chlorinated dianions. Weight loss is observed above 280 °C for $[C_4\text{mim}][C_2B_9H_{12}]$. The sample had lost 43% weight (117 g mol^{-1}) up to 600 °C.

(27) Masalles, C.; Llop, J.; Viñas, C.; Teixidor, F. *Adv. Mater.* **2002**, *14*, 826–829.
(28) Bradley, A. E.; Hardacre, C.; Holbrey, J. D.; Johnston, S.; McMath, S. E. J.; Nieuwenhuyzen, M. *Chem. Mater.* **2002**, *14*, 629–635.
(29) Bowlas, C. J.; Bruce, D. W.; Seddon, K. R. *Chem. Commun.* **1996**, 1625–1626.
(30) Binnemans, K. *Chem. Rev.* **2005**, *105*, 4148–4204.
(31) Gordon, J. E.; SubbaRao, G. N. *J. Am. Chem. Soc.* **1978**, *100*, 7445–7454.
(32) MacFarlane, D. R.; Seddon, K. R. *Aust. J. Chem.* **2007**, *60*, 3–5.

The TGA conditions for this compound were mimicked up to 400 °C for a 150 mg sample in a glassware setup. The nonvolatile part of the sample remained as a black solid, insoluble in water, propanone, *N*,*N*-dimethylmethanamide, and trichloromethane. The volatile decomposition products were condensed as a yellow oil and were scarcely soluble in trichloromethane but readily soluble in propanone. Neutral and anionic boron clusters were detected from this oil by means of ^{11}B NMR measurements (actual $^{11}B\{^1H\}$ NMR spectrum given as Supporting Information). To identify these decomposition products, further experiments are being considered.

$[C_4mim][Co(C_2B_9H_{11})_2]$ is more thermally stable, showing a small weight loss of only 5.8% (27 g mol^{-1}) between 340 and 700 °C. This value is close to a presumable ethene release (28.05 g mol^{-1}), although further TGA-MS (among other) experiments will be performed in our laboratories to gain more precise information about the decomposition products.

$[C_2mim]_2[B_{10}Cl_{10}]$ and $[C_{18}mim]_2[B_{10}Cl_{10}]$ started to decompose at ∼440 and ∼380 °C, respectively. The highest decomposition temperature found was that of $[C_2mim]_2[B_{12}Cl_{12}]$, which remained stable up to 480 °C. These salts with chlorinated dianions show a progressive weight decrease through the whole temperature scan (up to 1000 °C).

Comparing with data from literature, decomposition temperatures for alkylimidazolium salts follow the order $Cl^- < I^- < [C_2B_9H_{12}]^- < [PF_6]^- < [Co(C_2B_9H_{11})_2]^- < [BF_4]^- < [(CF_3SO_2)_2N]^- \sim [B_{10}Cl_{10}]^{2-} < [B_{12}Cl_{12}]^{2-}$.[3,5,33] The decomposition mechanism for 1-alkylimidazolium salts is likely to occur via S_N2 attack by the anion. Therefore, anions of low nucleophilicity produce more thermally stable salts. It appears that the tendency to react is greater for $[C_2B_9H_{12}]^-$ than for $[Co(C_2B_9H_{11})_2]^-$, but much less for $[B_{10}Cl_{10}]^{2-}$ and $[B_{12}Cl_{12}]^{2-}$. The salts obtained in this study with $[B_{12}Cl_{12}]^{2-}$ have the highest recorded decomposition temperature for alkylimidazolium compounds. The extremely high thermal stability of $Cs_2[B_{12}Cl_{12}]$ (>700 °C) was investigated in 1964 by Knoth et al.[34]

Density and Viscosity. The room temperature ionic liquids obtained in this work, $[C_nmim][Co(C_2B_9H_{11})_2]$ with n = 4, 6, 8, 10, 12, or 14 were obtained as red viscous liquids. To have an insight in their physical properties, density and viscosity measurements were recorded at different temperatures for one representative example, $[C_{12}mim][Co(C_2B_9H_{11})_2]$ (Figure 5). For increasing temperatures from 20 to 90 °C, the density of $[C_{12}mim][Co(C_2B_9H_{11})_2]$ decreases linearly in a short-range, from 1.085 to 1.035 g cm^{-3}, the temperature coefficient being −0.7081 mg cm^{-3} K^{-1},

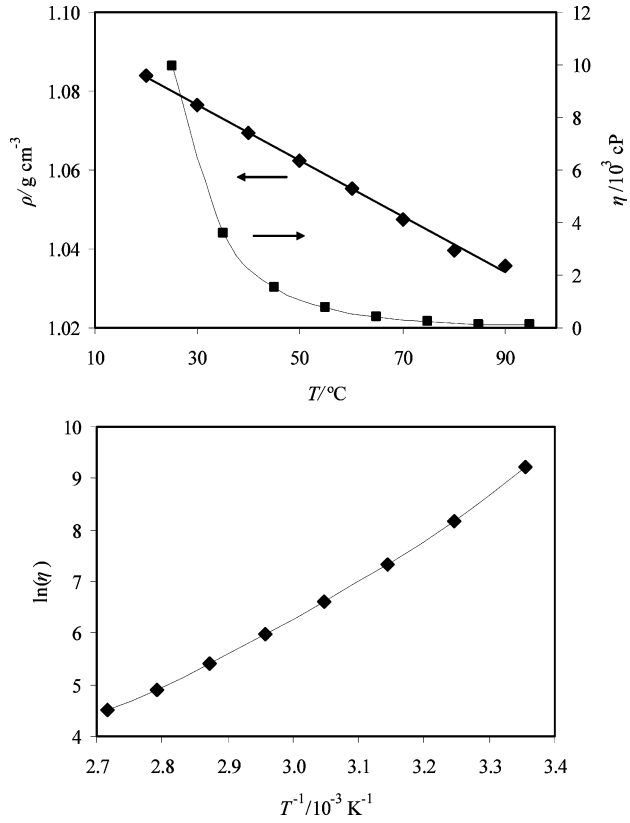

Figure 5. Density and viscosity plots for $[C_{12}mim][Co(C_2B_9H_{11})_2]$. Upper graph: Dependence on temperature. Lower graph: Arrhenius plots for viscosity are not linear; they rather fit the Vogel−Fülcher−Tammann equation.

comparable to that of other imidazolium salts.[35,36] This behavior is usual for ionic liquids.[21,37]

There exists a drastic dependence of viscosity upon temperature for the liquid salts $[C_nmim][Co(C_2B_9H_{11})_2]$ with n = 4, 6, 8, 10, 12, or 14. The viscosity of $[C_{12}mim][Co(C_2B_9H_{11})_2]$ at 25 °C is extremely high (9950 cP), but decreases markedly with temperature increase (Figure 5), being 2 orders of magnitude lower at 95 °C (91.3 cP). Arrhenius plots of the viscosity do not follow a straight line but are slightly curved. The values fit the Vogel−Fülcher−Tammann equation (1)[35,38]

$$\ln(\eta) = \ln(\eta_o) + B/(T - T_o) \quad (1)$$

where η_o = 0.0629 cP, B = 1290 K, and T_o = 190 K (R^2 = 0.9999).[39] The viscosity of an ionic liquid can vary with electrostatic forces, molecular weight of the ions, hydrogen bonding, Van der Waals interactions, or geometry of cation

(33) (a) Huddleston, J. G.; Visser, A. E.; Reichert, W. M.; Willauer, H. D.; Broker, G. A.; Rogers, R. D. *Green Chem* **2001**, *3*, 156–164. (b) Ngo, H. L.; LeCompte, K.; Hargens, L.; McEwen, A. B. *Thermochim. Acta* **2000**, *357*, 97–102.

(34) Knoth, W. H.; Miller, H. C.; Sauer, J. C.; Balthis, J. H.; Chia, Y. T.; Muetterties, E. L. *Inorg. Chem.* **1964**, *3*, 159–167.

(35) Fannin, A. A.; Floreani, D. A.; King, L. A.; Landers, J. S.; Piersma, B. J.; Stech, D. J.; Vaughn, R. L.; Wilkes, J. S.; Williams, J. L. *J. Phys. Chem.* **1984**, *88*, 2614–2621.

(36) Seddon, K. R.; Stark, A.; Torres, M. J. In *Clean Solvents: Alternative Media for Chemical Reactions and Processing*; Abraham, M., Moens, L., Eds.; American Chemical Society: Washington, DC, 2002; Vol. *819*, pp 34−49.

(37) Noda, A.; Hayamizu, K.; Watanabe, M. *J. Phys. Chem. B* **2001**, *105*, 4603–4610.

(38) Tammann, G.; Hesse, W. Z. *Z. Anorg. Allg. Chem.* **1926**, *156*, 245–257.

(39) The data also fit, not surprisingly, the modified Vogel−Fülcher−Tammann equation, $\ln(\eta) = \ln(\eta_o) + B/(T - T_o) + {}^1/_2 \ln(T)$, but no further improvement was achieved in the goodness of fit (R^2 = 0.9999).

Table 2. ^{11}B NMR Chemical Shifts (ppm, Relative to External $BF_3 \cdot Et_2O$) and Coupling Constants (Hz) of Representative Salts, in Propanone-d_6[a]

$[C_{18}mim][Co(C_2B_9H_{11})_2]$	$[C_{18}mim][C_2B_9H_{12}]$	$[C_{18}mim]_2[B_{12}Cl_{12}]$	$[C_{18}mim]_2[B_{10}Cl_{10}]$
6.1, 2 B, d, $^1J_{BH}$ = 133, B(8,8′)	−10.6, 2 B, d, $^1J_{BH}$ = 135, B(9,11)	−11.8, 12 B, s	−2.4, 2 B, s, B(1,10)
2.5, 2 B, d, $^1J_{BH}$ = 135, B(10,10′)	−16.6, 3 B, d, $^1J_{BH}$ = 145, B(3,5,6)		−9.6, 8 B, s, B(2−9)
−5.1, −5.8, 8 B, m, B(4,4′,7,7′,9,9′,12,12′)	−21.2, 2 B, d, $^1J_{BH}$ = 148, B(2,4)		
−16.4, 4 B, d, $^1J_{BH}$ = 156, B(5,5′,11,11′)	−32.7, 1 B, dd, $^1J_{BH(t)}$ = 133, $^1J_{BH(b)}$ = 23, B(10)		
−21.8, 2 B, br, B(6,6′)	−37.3, 1 B, d, $^1J_{BH}$ = 136, B(1)		

[a] See Chart 1 for numbering of boron cluster anions. In $[C_2B_9H_{12}]^-$, H(t) and H(b) indicate terminal and bridging hydrogen nuclei, respectively.

and anion.[1,5,37,40] Thus, it is not trivial to predict viscosities of ionic liquids from their compositions. As the cobaltabis(dicarbollide) anion is largely charge-dispersed[27] and, consequently, weakly coordinating, the high viscosity of $[C_{12}mim][Co(C_2B_9H_{11})_2]$ cannot be explained by Coulombic interactions or hydrogen bonding strength. Van der Waals forces between alkyl chains may contribute to this behavior, but most probably, the large size and molecular weight of the anion are closely related to the high viscosity, as has been shown elsewhere.

NMR Measurements. An extensive study on ^{1}H, $^{13}C\{^1H\}$, and ^{11}B nuclear magnetic resonance of the imidazolium boron cluster anion salts has been undertaken (see Supporting Information). The ^{11}B NMR spectra recorded for the novel salts agree with the structures of the clusters. Assigned ^{11}B NMR chemical shifts for selected salts of the four different boron cluster anions used in this work are listed in Table 2. ^{1}H NMR measurements have been taken for salts with the four anions studied, in different solvents, and at different concentrations. ^{1}H NMR chemical shifts show changes as a function of all these parameters (Figures 6 and 7, and Supporting Information).

Two main phenomena have been supposed to affect these shifts: hydrogen bonding and π-stacking.[5] It is assumed that hydrogen bonding causes a low field chemical shift of the proton.[41] This effect is observed for the aromatic acidic hydrogen atoms in imidazolium cations, that is, H(4), H(5), and especially H(2). At identical concentrations in the same solvent, their chemical shifts increase with anion hydrogen bond acceptor ability.[5,20] Thus, whereas H(2) chemical shifts fall in the range of 9.5−11.0 ppm for salts with good hydrogen bond acceptor anions, such as halides or carboxylates, they are below 9.1 ppm for all the newly synthesized salts presented here. This is accounted for by the low basicity of boron cluster anions. Similar ^{1}H NMR values have been documented for other weakly coordinating anions, such as $[NTf_2]^-$,[5] $[OTf]^-$,[5] $[BF_4]^-$,[3] or carborane anions.[14,17]

Although low field shifts should be larger for higher concentrations, the effect is the opposite for some imidazolium salts. This is explained by a model in which the ion pairs stack in solution in solvents of low polarity, with the rings parallel and staggered (Figure 8). The hydrogen atoms around the imidazolium rings enter the shielding cones above and below the neighboring rings, resulting in a high field shifting of their NMR signals.[5,20]

As for other imidazolium salts with weakly coordinating anions,[42] ^{1}H chemical shifts of these compounds at identical concentrations are solvent dependent (see Table 3 and Supporting Information). This effect is noticeable for all

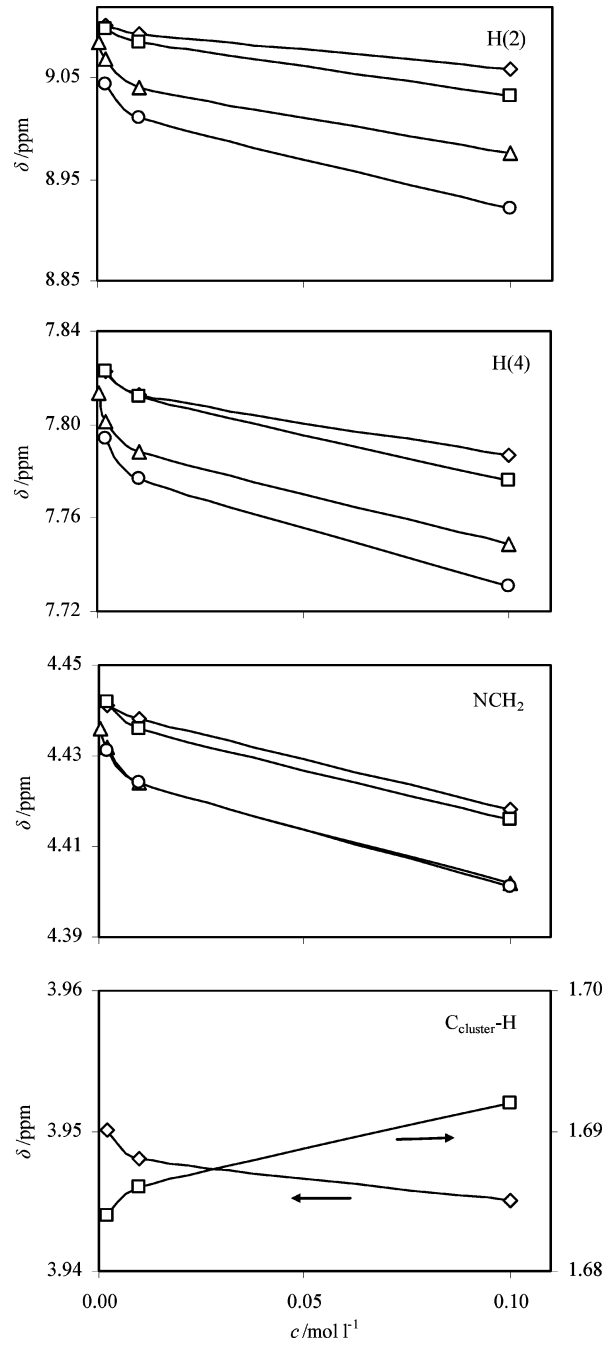

Figure 6. ^{1}H NMR chemical shifts of $[C_2mim]^+$ salts with the anions $[Co(C_2B_9H_{11})_2]^-$ (◇), $[C_2B_9H_{12}]^-$ (□), $[B_{12}Cl_{12}]^{2-}$ (Δ), and $[B_{10}Cl_{10}]^{2-}$ (○) as a function of the concentration, in propanone-d_6.

(40) Wasserscheid, P.; Keim, W. *Angew. Chem., Int. Ed.* **2000**, *39*, 3773–3789.

(41) Harris, R. K. *Nuclear Magnetic Resonance Spectroscopy*; Pitman Books Limited: London, 1983.

(42) (a) Headley, A. D.; Kotti, S.; Nam, J.; Li, K. Y. *J. Phys. Org. Chem.* **2005**, *18*, 1018–1022. (b) Headley, A. D.; Jackson, N. M. *J. Phys. Org. Chem.* **2002**, *15*, 52–55.

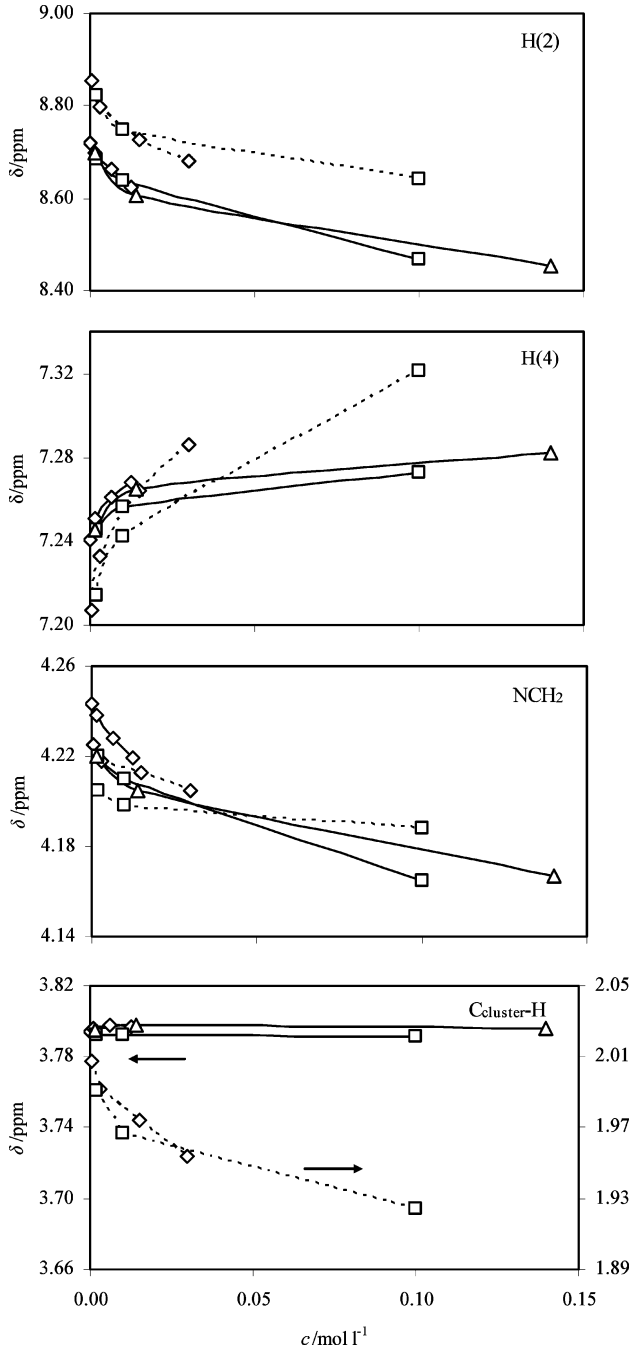

Figure 7. ^{1}H NMR chemical shifts of $[C_4mim][C_2B_9H_{12}]$ (···◇···), $[C_{14}mim][C_2B_9H_{12}]$ (···□···), $[C_4mim][Co(C_2B_9H_{11})_2]$ (−◇−), $[C_{14}mim][Co(C_2B_9H_{11})_2]$ (−□−), and $[C_{18}mim][Co(C_2B_9H_{11})_2]$ (−Δ−) as a function of the concentration, in $CDCl_3$.

hydrogen atoms in the cation (with the exception of alkyl protons beyond the β position from nitrogen), and also for $C_{cluster}$−H in $[Co(C_2B_9H_{11})_2]^-$, which experience low field shifts in propanone-d_6 compared to those in $CDCl_3$. This is caused by the greater ability of the former solvent to hydrogen bond to the above-mentioned relatively acidic hydrogen atoms. The opposite effect is observed for $C_{cluster}$−H in $[C_2B_9H_{12}]^-$.

^{1}H chemical shifts of $[C_2mim]^+$ salts with the four boron cluster anions used in this work have been measured in propanone-d_6 (Figure 6). Imidazolium protons experience high field shifts with increasing concentrations. Regardless

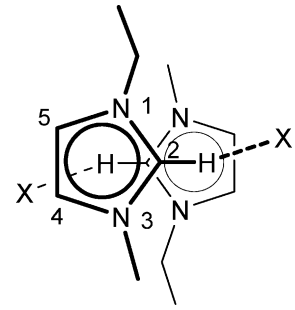

Figure 8. Proposed model for the stacking of ion pairs of $[C_2mim]X$ salts in solution and atom numbering in the imidazolium cation. Dashed lines indicate hydrogen bonds involving H(2).[20]

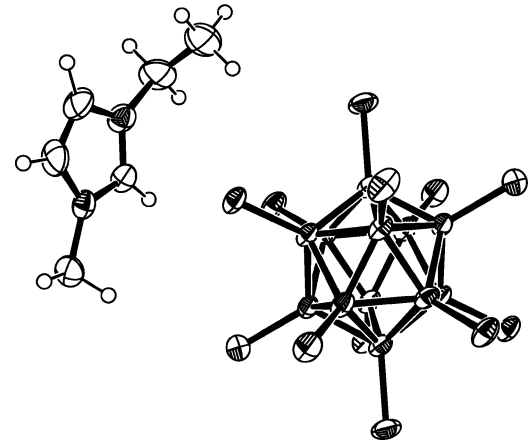

Figure 9. ORTEP drawing of the asymmetric unit of $[C_2mim]_2[B_{12}Cl_{12}]$. Thermal ellipsoids drawn at the 50% probability level.

of the anion, the effect decreases in the series $H(2) > H(4) \approx H(5) > NCH_2 \approx NCH_3 > NCH_2CH_3$ (see Supporting Information). This is behavior previously observed for salts of poor hydrogen bond acceptor anions in polar solvents.[5] Resonances of $C_{cluster}$−H in $[Co(C_2B_9H_{11})_2]^-$ are shifted to high field at high concentrations, as for the imidazolium protons, but with small shifts. However, these $C_{cluster}$−H resonances shifted in the opposite direction for $[C_2B_9H_{12}]^-$.

Samples of $[C_nmim][C_2B_9H_{12}]$ and $[C_nmim][Co(C_2B_9H_{11})_2]$ in $CDCl_3$ solutions were also analyzed as a function of the concentration. All the protons in $[C_nmim]^+$ except H(4) and H(5) show upfield shifts as the concentration is increased, but comparatively much larger for H(2) (see Figure 7 and Supporting Information). A parallel situation is the one reported for $[C_2mim]X$ (X = halide) in CD_2Cl_2 and was interpreted as an ordered π-stacking of ion pairs through the C(2) atoms of the imidazolium ring (see Figure 8);[20] H(4) and H(5) are believed to lay outside the shielding cones of the neighboring rings and remain only influenced by hydrogen bond strengthening.[5,20] Small variations in the chemical shifts of H(4) and H(5) in $[C_nmim][C_2B_9H_{12}]$ and $[C_nmim][Co(C_2B_9H_{11})_2]$ as a function of the concentration are observed, as expected by the poor hydrogen bond acceptor ability of the anions. Nonetheless, the somewhat larger variation for $[C_2B_9H_{12}]^-$ salts (0.06−0.11 ppm) compared to that of the $[Co(C_2B_9H_{11})_2]^-$ salts (0.02−0.04 ppm) suggest that, although extremely weak, hydrogen bonds could be slightly stronger in the former case. The chemical shifts of $C_{cluster}$−H and B−H−B of $[C_2B_9H_{12}]^-$ show

Table 3. ^{1}H NMR Chemical Shifts (ppm, Relative to $SiMe_4$) of Representative salts in 10^{-2} M Solutions in Propanone-d_6 and $CDCl_3$[a]

	$[C_{12}mim][Co(C_2B_9H_{11})_2]$			$[C_{12}mim][C_2B_9H_{12}]$		
	δ(propanone-d_6)	$\delta(CDCl_3)$	δ(propanone-d_6) − $\delta(CDCl_3)$	δ(propanone-d_6)	$\delta(CDCl_3)$	δ(propanone-d_6) − $\delta(CDCl_3)$
H(2)	9.09	8.64	+0.45	9.08	8.74	+0.34
H(4)	7.80	7.27	+0.53	7.80	7.24	+0.56
H(5)	7.75	7.27	+0.48	7.74	7.24	+0.50
NCH_2	4.39	4.21	+0.18	4.39	4.20	+0.19
NCH_3	4.09	4.01	+0.08	4.09	3.99	+0.10
NCH_2CH_2	1.97	1.91	+0.06	1.97	1.91	+0.06
$N(CH_2)_{11}CH_3$	0.87	0.88	−0.01	0.87	0.88	−0.01
$C_{cluster}H$	3.95	3.80	+0.15	1.69	1.97	−0.28

[a] The difference between these values is also shown.

Table 4. Dominant Infrared Bands above 3000 cm^{-1}[a]

	method	νC(4)-H, νC(5)-H		νC(2)-H		$\nu C_{cluster}$-H
$[C_2mim][Co(C_2B_9H_{11})_2]$	KBr pellet	3157(m)	3144(w)		3096(m)	3034(m)
	ATR	3158 (m)		3096 (m)		3034(m)
$[C_4mim][Co(C_2B_9H_{11})_2]$	KBr pellet	3159(m)	3148(m)	3115(m)	3099(m)	3038(m)
	liquid on NaCl	3159 (s)	3148 (s)	3117(m)	3099(m)	3040(m)
	ATR	3146 (m)		3115(m)	3099(m)	3038(m)
$[C_6mim][Co(C_2B_9H_{11})_2]$	KBr pellet	3159(m)	3150(m)	3115(m)	3099(m)	3040(m)
	liquid on NaCl	3159 (s)	3148 (s)	3115 (s)	3099(m)	3040(m)
$[C_8mim][Co(C_2B_9H_{11})_2]$	KBr pellet	3161(w)	3148(m)	3115(m)	3099(m)	3040(m)
	liquid on NaCl	3159 (s)	3148 (s)	3117(m)	3099(m)	3040(m)
$[C_{10}mim][Co(C_2B_9H_{11})_2]$	KBr pellet	3159(w)	3146(m)	3115(m)	3099(m)	3040(m)
	liquid on NaCl	3159(m)	3148 (s)	3115(m)	3099(m)	3040(m)
$[C_{12}mim][Co(C_2B_9H_{11})_2]$	KBr pellet	3159(w)	3148(m)	3117(m)	3097(m)	3040(m)
	liquid on NaCl	3159(m)	3150 (s)	3117(m)	3099(m)	3040(m)
	ATR	3146 (m)		3115(m)	3099(m)	3038(w)
$[C_{14}mim][Co(C_2B_9H_{11})_2]$	KBr pellet	3159(w)	3148(m)	3117(m)	3097(m)	3040(m)
	liquid on NaCl	3159(m)	3147 (s)	3117 (s)	3097(m)	3040(m)
$[C_{16}mim][Co(C_2B_9H_{11})_2]$	KBr pellet	3165(m)	3148(w)	3107 (m)		3036(w)
	ATR	3164 (m)		3108 (m)		3035(w)
$[C_{18}mim][Co(C_2B_9H_{11})_2]$	KBr pellet	3163(m)	3146(m)	3107 (m)		3036(w)
$[C_2mim][C_2B_9H_{12}]$	KBr pellet	3162(m)	3148(m)	3119 (m)		3032(w)
	ATR	3162(w)	3147(m)	3122 (m)		*b*
$[C_4mim][C_2B_9H_{12}]$	KBr pellet	3157(m)	3146(w)	3115 (m)		3032(w)
$[C_6mim][C_2B_9H_{12}]$	KBr pellet	3160(m)	3146(w)	3119(m)		3032(w)
	ATR	3157(m)	3144(w)	3119 (m)		*b*
$[C_8mim][C_2B_9H_{12}]$	KBr pellet	3159(m)	3146(w)	3119 (m)		3028(w)
$[C_{10}mim][C_2B_9H_{12}]$	KBr pellet	3159(m)	3148(w)	3121 (m)		3028(w)
$[C_{12}mim][C_2B_9H_{12}]$	KBr pellet	3159(m)	3148(w)	3121 (m)		3028(w)
$[C_{14}mim][C_2B_9H_{12}]$	KBr pellet	3159(m)	3148(w)	3121 (m)		3028(w)
	ATR	3159 (m)		3120 (m)		*b*
$[C_{16}mim][C_2B_9H_{12}]$	KBr pellet	3159(m)	3148(w)	3121(m)		3028(w)
	ATR	3159 (m)		3120 (m)		*b*
$[C_{18}mim][C_2B_9H_{12}]$	KBr pellet	3159(m)	3148(w)	3121 (m)		3028(w)
$[C_2mim]_2[B_{10}Cl_{10}]$	KBr pellet	3165(m)	3151 (s)	3119(m)	3103(m)	
	ATR	3150 (m)		3118(m)	3103(w)	
$[C_{16}mim]_2[B_{10}Cl_{10}]$	KBr pellet	3159 (m)		3119 (m)		
	ATR	3157 (w)		3118 (w)		
$[C_{18}mim]_2[B_{10}Cl_{10}]$	KBr pellet	3157 (m)		3119 (m)		
$[C_2mim]_2[B_{12}Cl_{12}]$	KBr pellet	3165 (s)	3150(m)	3117 (m)		
	ATR	3165 (m)		3116 (m)		
$[C_8mim]_2[B_{12}Cl_{12}]$	KBr pellet	3157 (s)		3117 (m)		
$[C_{10}mim]_2[B_{12}Cl_{12}]$	KBr pellet	3159 (m)		3115 (m)		
$[C_{16}mim]_2[B_{12}Cl_{12}]$	KBr pellet	3155 (m)		3119 (m)		
	ATR	3153 (w)		3119 (w)		
$[C_{18}mim]_2[B_{12}Cl_{12}]$	KBr pellet	3165 (m)		3119 (w)		

[a] C−H stretching frequencies in cm^{-1}. [b] Bands are too small and broad, so that absorption maxima could not be unambiguously determined.

noticeable upfield shifts with increasing concentration (see Supporting Information), indicating that close contacts are probably being established between the open face of the nido-anion and the molecular plane of the imidazolium ring.

Infrared Spectroscopy. Dominant infrared bands for the reported imidazolium-boron cluster anion salts observed above 3000 cm^{-1} are listed in Table 4. The room temperature ionic liquid salts ($[C_nmim][Co(C_2B_9H_{11})_2]$ with $n = 4$, 6, 8, 10, 12, or 14) were analyzed as thin layers over NaCl discs. Furthermore, FT-IR/ATR experiments were carried out for some selected samples. For a given salt, band frequencies do not experience noticeable variations when comparing data from KBr pellets with those from neat liquids or reflectance measurements (<3 cm^{-1} in most cases). Thus, no ionic exchange is expected to occur in the pressed pellets, probably because of immiscibility between imidazolium-boron cluster anion salts and KBr.

The H(2) hydrogen atom is the most acidic one in the ring, thus most prone to hydrogen bonding (see Supporting Information for actual spectra). The stretching frequencies of the C(2)−H(2) bond fall within 3121 and 3096 cm^{-1}. The higher frequency bands are assigned[43,44] to the C(4)−H(4) and C(5)−H(5) stretches; two peaks are often observed between 3165 and 3146 cm^{-1}. All these data are close to

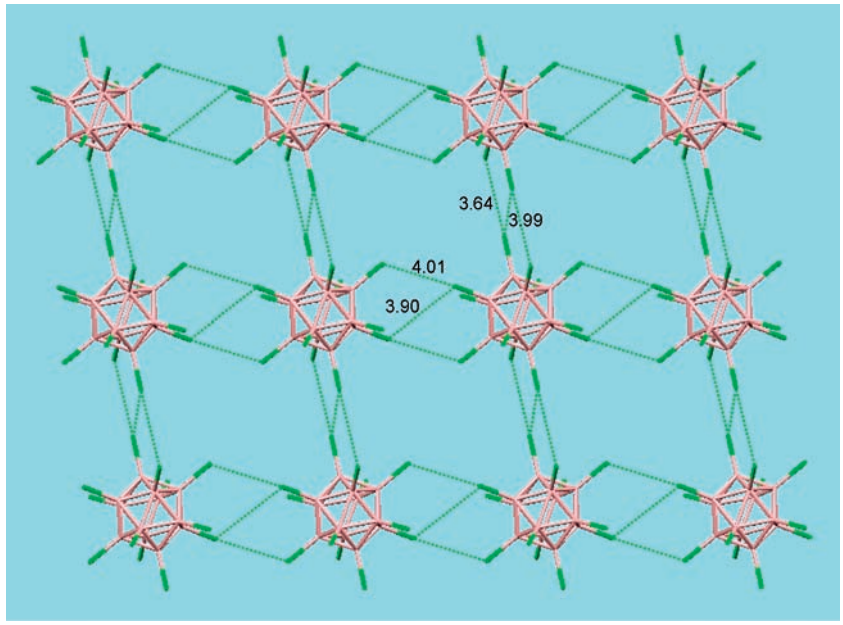

Figure 10. Packing of anions into layers in $[C_2mim]_2[B_{12}Cl_{12}]$ showing the Cl···Cl contacts (distances in Å). Boron = pink, chlorine = green.

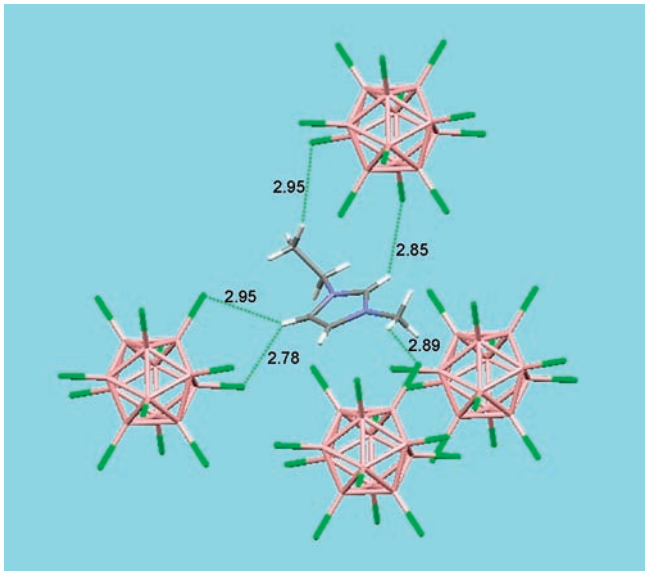

Figure 11. Pseudotetrahedral coordination of anions around a cation in the crystal structure of $[C_2mim]_2[B_{12}Cl_{12}]$ showing the closest H···Cl (distances in Å). Boron = pink, chlorine = green, carbon = gray, nitrogen = blue, hydrogen = white.

Table 5. Average Distances (Å) and their Standard Deviations (ASD) for $[B_{12}X_{12}]^{2-}$ Salts

X	*d*(B−B)	ASD	d(B-X)	ASD	ref
F	1.78	0.0116	1.39	0.0087	49
Cl	1.79	0.0080	1.79	0.0096	47, this paper
Br	1.78	0.0147	1.95	0.0119	47, 50
I	1.79	0.0206	2.15	0.0212	47, 51

the ones reported for imidazolium salts with [*closo*-$CB_{11}H_{12}]^-$ derivatives[14] or [1-R-*closo*-$SnB_{11}H_{11}]^-$,[15] (3128−3093 cm^{-1} for C(2)−H(2)) but substantially higher than those of the halides (3080−3052 cm^{-1} for C(2)−H(2)),[44] suggesting that if hydrogen bonds exist here, they are extremely weak. The small range of frequencies (19 cm^{-1} for C(4)−H(4) and C(5)−H(5), and 26 cm^{-1} for C(2)−H(2) stretches) suggests that the strength of interactions involving aromatic imidazolium protons vary only in a trivial manner when changing the anion and/or the alkyl chain length.

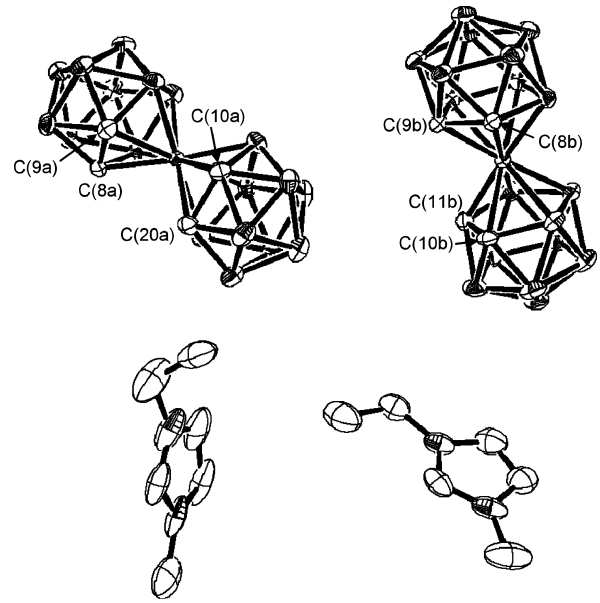

Figure 12. ORTEP drawing of the asymmetric unit of $[C_2mim][Co(C_2B_9H_{11})_2]$. Thermal ellipsoids drawn at the 50% probability level. Hydrogen atoms omitted for clarity.

In the spectra of the salts with $[Co(C_2B_9H_{11})_2]^-$ or $[C_2B_9H_{12}]^-$ anions, $C_{cluster}$−H stretches are also present. For the *nido*-carborane anion $[C_2B_9H_{12}]^-$ they appear as weak (often barely observed) bands between 3032 and 3025 cm^{-1}. More intense bands are observed for the cobaltabis(dicarbollide) anion, in the frequency range of 3040−3034 cm^{-1}. The bands related to B−H stretches are strong bands between 2600 and 2500 cm^{-1}. All these data are close to the ones observed for other carborane or stannaborane salts.[14,15]

(43) Tait, S.; Osteryoung, R. A. *Inorg. Chem.* **1984**, *23*, 4352–4360.
(44) Elaiwi, A.; Hitchcock, P. B.; Seddon, K. R.; Srinivasan, N.; Tan, Y. M.; Welton, T.; Zora, J. A. *J. Chem. Soc., Dalton Trans.* **1995**, 3467–3472.

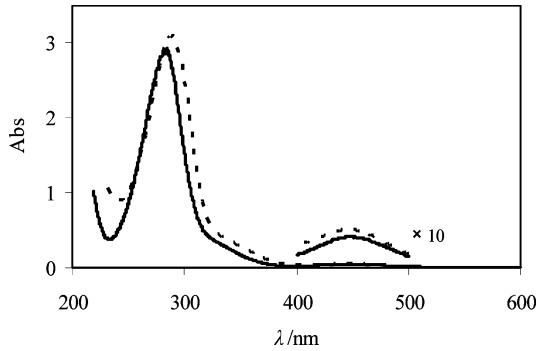

Figure 13. UV−visible absorption spectra of $[C_{12}mim][Co(C_2B_9H_{11})_2]$ in ethanenitrile (solid lines) and dichloromethane (dashed lines) solutions, measured in 1 mm path length cuvettes.

X-ray Structures. The asymmetric unit of $[C_2mim]_2[B_{12}Cl_{12}]$ contains one ion pair (Figure 9). Within the crystal structure, the anions pack such that they form layers (Figure 10) in the *ab* plane with cavities. The layers can be thought of as the result of Cl···Cl close contacts, 3.64 Å being the closest. These contacts are, not surprisingly, above the sum of van der Waals radii, which is 3.50 Å, according to Bondi's statistical study on molecular crystals.[45] Nevertheless, one has to take into account the presumably longer Van der Waals radii in negatively charged species.[46] The cations lay within the cavities, with a pseudotetrahedral coordination of anions (Figure 11); probably oriented by the sum of weak hydrogen interactions between the ring, methyl, and ethyl protons with the chlorine atoms that are not involved in the anion layers. The closest hydrogen bonded contact is with the H(4) at 2.78 Å, rather that the more acidic H(2) at 2.85 Å.

Just a few examples of crystal structures containing other dodecahalododecaborane dianions ($[B_{12}X_{12}]^{2-}$) have been published.[47−51] The average bond distances and standard deviations for all these salts are listed in Table 5, showing that the effect of the change of exo-cluster halogen has little or no influence on B−B distances. B−X distances increase in the order $F < Cl < Br < I$, as expected.

The asymmetric unit of $[C_2mim][Co(C_2B_9H_{11})_2]$ (Figure 12) contains two anions and two cations that form alternating cation−anion stacks. There are no significant interactions between the ions other than electrostatic, and hydrogen bonds seem to be extremely weak or absent. Bond distances within the cluster fall in the usual range for this anion,[52] on the basis of statistical analysis from the Cambridge Structural Database.

Electronic Absorption Spectroscopy. Absorption spectra of $[C_{12}mim][Co(C_2B_9H_{11})_2]$ have been recorded in 10^{-3} M ethanenitrile and dichloromethane solutions between 200 and 600 nm. Two maxima can be distinguished, with small variation between solvents (Figure 13). Frequencies and extinction coefficients are as follows: λ/nm = 289 (31100 L mol^{-1} cm^{-1}), 446 (512 L mol^{-1} cm^{-1}) in ethanenitrile and 285 (29400 L mol^{-1} cm^{-1}), 448 (410 L mol^{-1} cm^{-1}) in dichloromethane. These two absorptions have been reported to be due to electronic transitions in the cobaltabis(dicarbollide) anion.[53,54] A shoulder is observed over 300 nm, which has previously been attributed also to the $[Co(C_2B_9H_{11})_2]^-$ anion.[53]

Conclusions

Highly pure and nonhygroscopic boron cluster anion ionic liquids can be obtained by combining anions such as $[Co(C_2B_9H_{11})_2]^-$, $[C_2B_9H_{12}]^-$, $[B_{10}Cl_{10}]^{2-}$, or $[B_{12}Cl_{12}]^{2-}$ with either imidazolium or phosphonium cations in straightforward metathetic reactions. These materials are considerably viscous when melted, although viscosity dramatically decreases upon heating. One interesting property, provided by the inert and weakly coordinating nature of boron cluster anions, is the noticeable thermal resistance of their imidazolium salts. Especially high are the decomposition temperatures when the counteranion is the icosahedral $[B_{12}Cl_{12}]^{2-}$. Melting points (or glass transition temperatures, where appropriate) are clearly diminished by the presence of uncharged moieties, such as alkyl chains, attached to the charged parts of the ions. Alkyl chains both elongate interionic distances and add conformational freedom. Nevertheless, anions bearing widely delocalized charge are also responsible for lowering melting points. This is the case of $[Co(C_2B_9H_{11})_2]^-$. Even dianions, such as highly symmetrical $[B_{10}Cl_{10}]^{2-}$ and $[B_{12}Cl_{12}]^{2-}$ can produce room temperature ionic liquids or ionic liquid

(45) Bondi, A. *J. Phys. Chem.* **1964**, *68*, 441–451.
(46) (a) Desiraju, G. R. *Crystal Engineering. The Design of Organic Solids*; Elsevier: Amsterdam, 1989. (b) van den Berg, J. A.; Seddon, K. R. *Cryst. Growth Des.* **2003**, *3*, 643–661.
(47) Tiritiris, I.; Schleid, T. *Z. Anorg. Allg. Chem.* **2004**, *630*, 1555–1563.
(48) (a) Tiritiris, I.; Schleid, T. *Z. Anorg. Allg. Chem.* **2003**, *629*, 581–583. (b) Tiritiris, I.; Schleid, T. *Z. Anorg. Allg. Chem.* **2002**, *628*, 2212.
(49) (a) Ivanov, S. V.; Miller, S. M.; Anderson, O. P.; Solntsev, K. A.; Strauss, S. H. *J. Am. Chem. Soc.* **2003**, *125*, 4694–4695. (b) Solntsev, K. A.; Mebel, A. M.; Votinova, N. A.; Kuznetsov, N. T.; Charkin, O. P. *Koord. Khim.* **1992**, *18*, 340–364.
(50) Volkov, O.; Hu, C. H.; Paetzold, P. *Z. Anorg. Allg. Chem.* **2005**, *631*, 1107–1112.
(51) Tiritiris, I.; Schleid, T. *Z. Anorg. Allg. Chem.* **2001**, *627*, 2568–2570.
(52) (a) Sumby, C. J.; Fisher, J.; Prior, T. J.; Hardie, M. J. *Chem.—Eur. J.* **2006**, *12*, 2945–2959. (b) Mutseneck, E. V.; Starikova, Z. A.; Lyssenko, K. A.; Petrovskii, P. V.; Zanello, P.; Corsini, M.; Kudinov, A. R. *Eur. J. Inorg. Chem.* **2006**, 4519–4527. (c) Kazheva, O. N.; Chekhlov, A. N.; Alexandrov, G. G.; Buravov, L. I.; Kravchenko, A. V.; Starodub, V. A.; Sivaev, I. B.; Bregadze, V. I.; Dyachenko, O. A. *J. Organomet. Chem.* **2006**, *691*, 4225–4233. (d) Kašná, B.; Jambor, R.; Dostál, L.; Císařova, I.; Holeček, J.; Štíbr, B. *Organometallics* **2006**, *25*, 5139–5144. (e) Cunha-Silva, L.; Westcott, A.; Whitford, N.; Hardie, M. J. *Cryst. Growth Des.* **2006**, *6*, 726–735. (f) Bachmann, J.; Nocera, D. G. *J. Am. Chem. Soc.* **2005**, *127*, 4730–4743. (g) Rossmeier, T.; Korber, N. Z. *Anorg. Allg. Chem.* **2004**, *630*, 2665–2668. (h) Polyanskaya, T. M.; Volkov, V. V.; Drozdova, M. K. *J. Struct. Chem.* **2003**, *44*, 632–641. (i) Plešek, J.; Backovsky, J.; Císařova, I. Private Communication to the Cambridge Structural Database, 2003. (j) Ahmad, R.; Hardie, M. J. *Cryst. Growth Des.* **2003**, *3*, 493–499. (k) Schweiger, M.; Seidel, S. R.; Arif, A. M.; Stang, P. J. *Inorg. Chem.* **2002**, *41*, 2556–2559. (l) Renard, S. L.; Franken, A.; Kilner, C. A.; Kennedy, J. D.; Halcrow, M. A. *New J. Chem.* **2002**, *26*, 1634–1637. (m) Hardie, M. J.; Raston, C. L.; Salinas, A. *Chem. Commun.* **2001**, 1850–1851. (n) Hardie, M. J.; Malic, N.; Raston, C. L.; Roberts, B. A. *Chem. Commun.* **2001**, 865–866. (o) Polyanskaya, T. M.; Volkov, V. V.; Price, C.; Thornton-Pett, M.; Kennedy, J. D. *Khim. Interesach Ustoich. Razvit.* **2000**, *8*, 229. (p) Chamberlin, R. M.; Scott, B. L.; Melo, M. M.; Abney, K. D. *Inorg. Chem.* **1997**, *36*, 809–817. (q) Xie, Z. W.; Jelínek, T.; Bau, R.; Reed, C. A. *J. Am. Chem. Soc.* **1994**, *116*, 1907–1913. (r) Borodinsky, L.; Sinn, E.; Grimes, R. N. *Inorg. Chem.* **1982**, *21*, 1686–1689.
(53) Rojo, I.; Teixidor, F.; Viñas, C.; Kivekäs, R.; Sillanpää, R. *Chem.—Eur. J.* **2003**, *9*, 4311–4323.
(54) Hawthorne, M. F.; Young, D. C.; Andrews, T. D.; Howe, D. V.; Pilling, R. L.; Pitts, A. D.; Reintjes, M.; Warren, L. F.; Wegner, P. A. *J. Am. Chem. Soc.* **1968**, *90*, 879–896.

crystals, when the cation is carefully selected to be of low symmetry, for example, $[P_{6\,6\,6\,14}]_2[B_{10}Cl_{10}]$, which has a melting point of 53 °C. As suggested by ^{1}H NMR measurements of variable concentration solutions, $[C_2B_9H_{12}]^-$ can establish contacts with both the π system and the acidic protons of the imidazolium rings, whereas hydrogen bonding would be much weaker in $[C_n\text{mim}][Co(C_2B_9H_{11})_2]$ (if existing), because of the highly delocalized charge of the anion. With this assumption, the lattice energies would be in general higher for $[C_n\text{mim}][C_2B_9H_{12}]$, in turn explaining the large difference in melting points between $[C_n\text{mim}][C_2B_9H_{12}]$ and $[C_n\text{mim}][Co(C_2B_9H_{11})_2]$ (when $n = 4$, 6, 8, 10, 12, or 14).

Acknowledgment. This work was supported by CICYT (Project MAT2006-05339), Generalitat de Catalunya (2005/SGR/00709). A.V.P. thanks MEyC for a PhD grant. K.R.S. acknowledges the EPSRC (Portfolio Partnership Scheme, Grant EP/D029538/1) for support.

Supporting Information Available: Tables listing ^{1}H NMR chemical shifts in propanone-d_6 and in $CDCl_3$ at different concentrations, ^{13}C {^{1}H} NMR chemical shifts, CHN microanalysis data for the newly synthesized salts, viscosity and density data for $[C_{12}\text{mim}][Co(C_2B_9H_{11})_2]$ at different temperatures, ^{11}B and ^{11}B{^{1}H} NMR spectra of $[NH_4]_2[B_{12}Cl_{12}]$, ^{11}B{^{1}H} NMR spectrum of the volatile product from the thermal decomposition of $[C_4\text{mim}][C_2B_9H_{12}]$, ^{1}H and ^{13}C{^{1}H} NMR, and FT-IR spectra of selected samples. This material is available free of charge via the Internet at http://pubs.acs.org.

IC801448W